

BARRIER-HEIGHT AND HOT ELECTRON ATTENUATION LENGTH MEASUREMENTS IN Au—Si, Ag—Si AND Al—Si DIODES BETWEEN 280—350 K

By

B. PELLE¹, J. KISPÉTER², J. PEISZNER³

(Received October 31, 1983)

Schottky barrier diodes were prepared in chemically cleaned, 0.1 ohm-cm, n-type Si by evaporating Au, Ag and Al layers, respectively at $\sim 5 \cdot 10^{-8}$ mbar. Barrier heights of these diodes have been determined by standard $I-V$, $C-V$ and photoemission threshold measurements at various temperatures between 280—350 K. The same tendency has been observed using the different methods; a slow decrease of barrier height with temperature ($\sim -4 \cdot 10^{-4}$ eV/K). Special care was taken to determine the correct value of photoemission yield. Photoemission measurements proved to be the most reliable method to determine the barrier height but no significant discrepancies were observed in the results obtained by the photoemission, $I-V$ and $C-V$ methods.

Attenuation length L of hot electrons in Au, Ag and Al has been determined from measurement of the photoemission yield for various metallic layer thicknesses at different temperatures between 280—350 K. For Au layers an empirical relation of $T^{0.23}L(T) = \text{const}$ seems to be correct for 280—350 K.

1. Introduction

Metal-semiconductor contacts are of immense importance in contemporary electronic devices. Recently some interest has been shown in the use of metal-semiconductor barriers realized on Si for detection of infrared radiation and conversion of solar energy. This latter application suggested us to investigate the behaviour of Schottky barriers at temperatures above room temperature until 350 K.

Several authors have determined the electronic barrier height on different metal-silicon contacts by means of standard $I-V$, $C-V$ and photoemission threshold measurements [1, 3, 6, 7, 9, 10] and the hot electron attenuation length in metallic films [2—5, 8] at temperatures ranging between 80—300 K. However, no results have been reported at temperatures below the liquid nitrogen temperature and above room temperature.

¹ Université des Sciences et de la Technologie d'Oran (Algeria).

² College of Food Industry, Szeged, (Hungary).

³ Institut National Polytechnique de Grenoble (France).

2. Experimental

The silicon wafers used in our experiments were of $0.1 \text{ ohm}\cdot\text{cm}$, n -type ($N_D \sim 7 \cdot 10^{18} \text{ cm}^{-3}$), (111) oriented. They were etched in HNO_3 — HF (20:1) mixture, then immersed in cc. HNO_3 for a short time, rinsed in deionized H_2O and dried in H_2 flow. Oxide was removed from the bottom side with cc. HF , then the wafers were rinsed and dried again. Contacts were made by evaporating Al film then the wafers were tempered at 673 K in the vacuum system. For barrier preparation the front side of the wafers was rinsed in cc. HF to turn the surface into hydrophobic just before inserting the wafers into the vacuum system. Thin Au, Ag, or Al films were evaporated from W-boat through a stainless-steel mask having circular holes with diameters of 2 mm or 0.7 mm, respectively, at a pressure of $5 \cdot 10^{-8}$ mbar. Film thickness was monitored during deposition by a quartz crystal microbalance calibrated previously by Talystep and interference microscope.

For each evaporation process both a $10 \times 20 \text{ mm}^2$ Si wafer and a $10 \times 20 \text{ mm}^2$ fused silica plate were inserted to measure optical transmission, reflectivity and resistivity of the deposited metallic layers.

During $I-V$, $C-V$ and photoemission yield measurements at various temperatures (from 280 to 350 K) the slices were placed onto a gold plated vacuum thermochuck. Its temperature was regulated by a Temptronic electronic temperature controller. For the measurements a P.A.R. point probe assembly was used equipped with an $X-Y-Z$ micromanipulator. The vacuum thermochuck and the point probe assembly with the manipulator were inserted into a measuring box with removable cover, in which an optical window of Infrasil quality fused silica was mounted for photoemission measurements. For voltage supply a highly isolated voltage source was provided with 1.2 V Hg—Cd batteries and 10 turn precision Helipot potentiometers.

For $I-V$ measurements the applied voltage was monitored by a Keithley Mod 191 digital voltmeter and the current was measured by a Keithley Mod 616 digital electrometer (Fig. 1). The $C-V$ characteristics were measured by a P.A.R. Mod

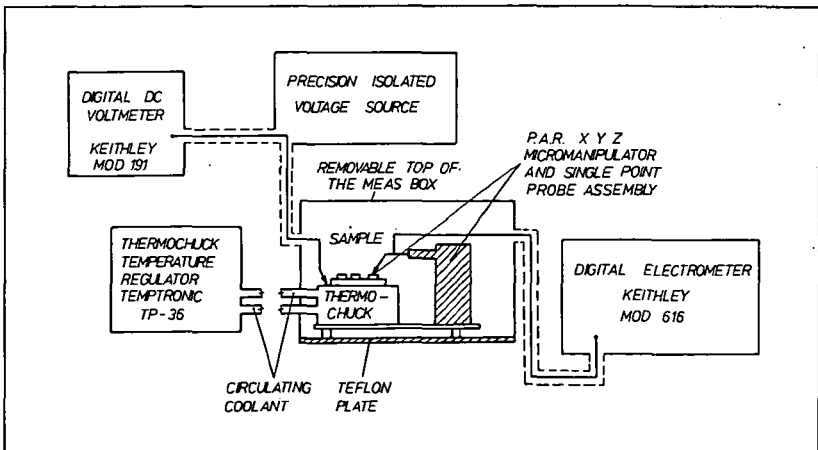


Fig. 1. Electrical circuit for $I-V$ characteristics measurements

410 hf $C-V$ plotter assembly operating at 1 kHz and were recorded by a SEFRAM TGM 164 $x-y$ recorder (Fig. 2).

Measuring circuitry and optical arrangement used for photoemission yield measurements are shown in detail in Fig. 3.

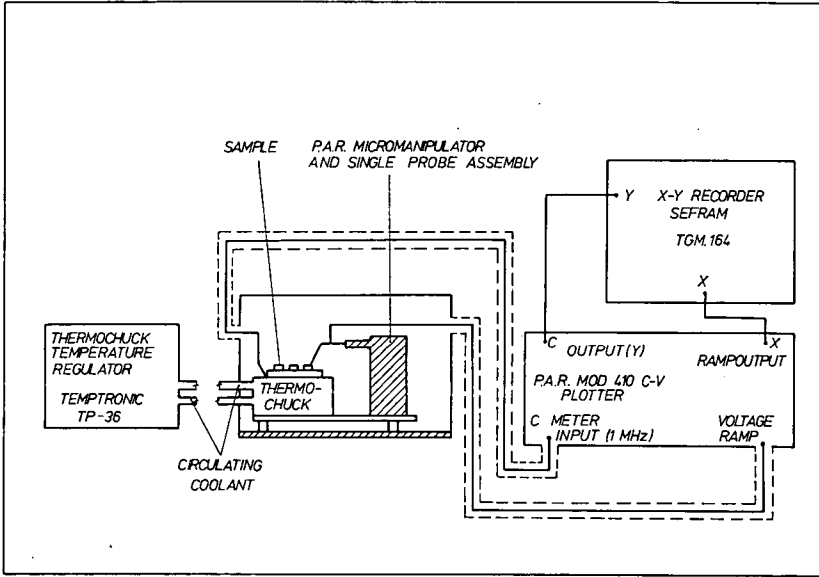


Fig. 2. Electrical circuit for $C-V$ characteristics measurements

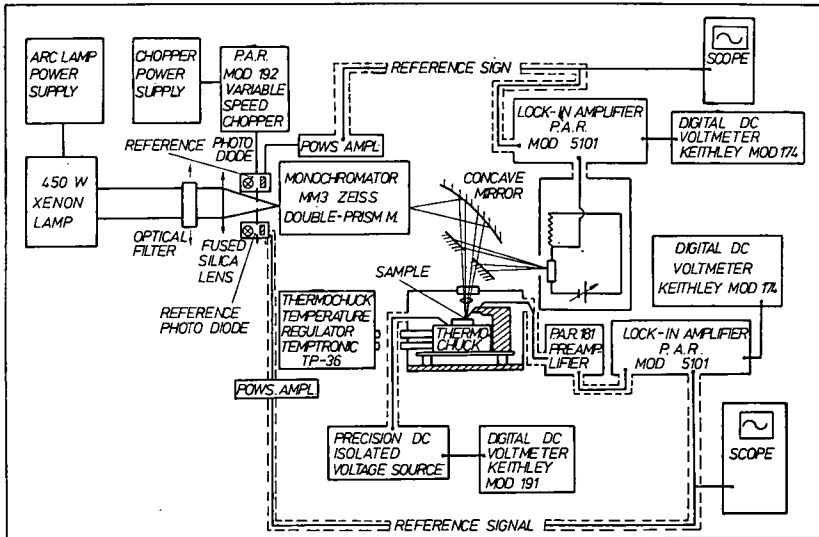


Fig. 3. Experimental arrangement for photoyield measurements

Since the photocurrents generated were relatively small (10^{-12} – 10^{-8} A), and thermoemission currents are in the range of 10^{-9} – 10^{-8} A at room temperature even at slight reverse bias (-0.5 V) applied for photoemission measurements, a.c. locking technique was used instead of a.c. measurements with electrometer. Light was chopped by a P.A.R. Mod 192 chopper at 239 Hz and the photocurrents were detected with P.A.R. Mod 5101 lock-in amplifier equipped with a P.A.R. Mod 181 current sensitive preamplifier. Currents ranging between 10^{-12} to 10^{-8} A could easily be detected by this assembly.

As a light source 450 W Xe arc lamp was used which was followed by a Zeiss MM3 double prism monochromator to select wavelengths. The chopped monochromatic light was focused onto the sample by a concave reflecting mirror and a fused silica lens. A part of the light was reflected onto the surface of a PbS detector. Photocurrent and incident photon flux could be measured at the same time by this assembly calibrated previously, so the photoresponse could be determined directly as a function of wavelength (or photon energy).

3. Experimental results

Barrier height determination

Schottky barrier heights were determined in three ways:

- a) "forward current I – V method": by plotting the logarithm of the forward current density versus applied bias, the barrier height was found from the intercept of the extrapolated current density curve on the current density axis.
- b) " C – V method": by plotting the reciprocal of the square of the differential capacitance C^{-2} versus applied reverse bias, barrier height was found from the intercept on the voltage axis.
- c) "photoresponse measurement": by plotting the square root of the photoelectric response (yield) $Y^{1/2}$ as a function of photon energy (Fowler-plot), the barrier height was found from the intercept of the extrapolated photoresponse curve on the photon energy axis.

Barrier height determination from I – V characteristics

For semiconductors with low doping concentration ($N_D; N_A < 10^{17}$ cm $^{-3}$) the I – V characteristics in forward direction between 280–350 K with $V > 3 kT/q$ can be given as

$$I = A^{**} T^2 \exp\left(\frac{-q\Phi_{B0}}{kT}\right) \exp\left(\frac{q(\Delta\Phi + V)}{kT}\right), \quad (1)$$

where I is the current density, A^{**} is the effective Richardson-constant, $q\Phi_{B0}$ is the zero field asymptotic barrier height, $\Delta\Phi$ is the Schottky barrier lowering, V is the applied bias. $q\Phi_{B0}$ was determined by plotting the I – V characteristics, with I in logarithmic scale.

The extrapolated value of current density to zero voltage gives the saturation current I_s :

$$I_s = A^{**} T^2 \exp\left(\frac{-q\Phi_{Bo}}{kT}\right) \quad (2)$$

and the barrier height can be given as

$$q\Phi_{Bo} = kT \ln\left(\frac{A^{**} T^2}{I_s}\right) \quad (3)$$

$A^{**} = 105 \text{ Acm}^{-2} \text{ K}^{-2}$ was assumed throughout this work.

In reality, the diode equation is as follows:

$$I = I_s \left\{ \exp\left(\frac{qV}{nkT}\right) - 1 \right\}, \quad (4)$$

where n is the "ideality factor" which can be determined from

$$n = \frac{q}{kT} \frac{\partial V}{\partial(\ln I)}. \quad (5)$$

Figs. 4, 5 and 6 represent our experimental $I-V$ curves obtained at various temperatures between 280–350 K for nSi(111)—Au, nSi(111)—Al and nSi(111)—Ag diodes fabricated with chemically cleaned Si-surfaces.

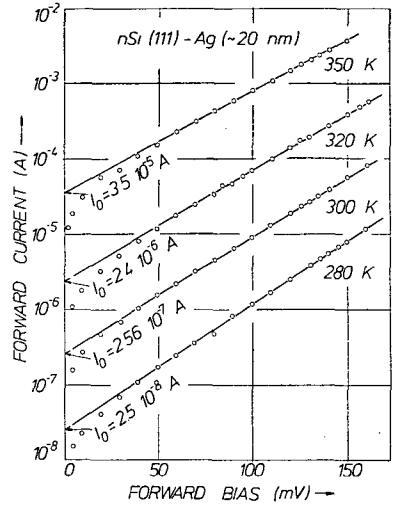


Fig. 4. Forward current-voltage characteristics of nSi(111)—Au (20 nm) diodes for various temperatures (280, 300, 320 and 350 K)

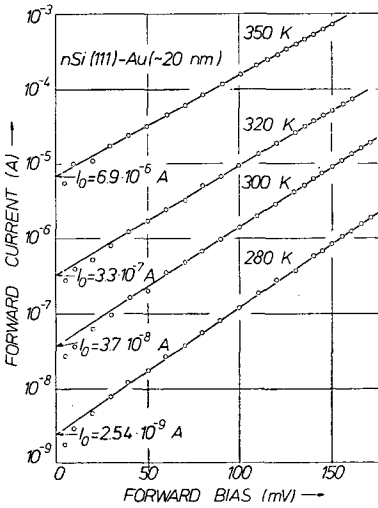


Fig. 5. Forward current-voltage characteristics of nSi(111)—Al (25 nm) diodes for 280, 300, 320 and 350 K

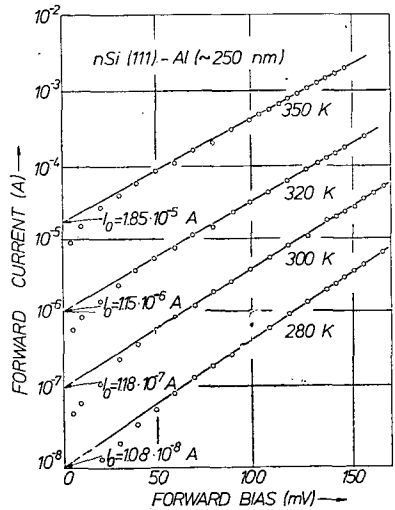


Fig. 6. Forward current-voltage characteristics of n-Si(111)—Ag (20 nm) diodes at 280, 300, 320 and 350 K

Table I

Barrier heights of *n* type Si (111) — metallic layer diodes with $N_D = 7 \cdot 10^{16} \text{ cm}^{-3}$ from *I*—*V* measurements at various temperatures

Temperature (K)	Au—Si $q\Phi_{Bo}$ (eV)	Al—Si $q\Phi_{Bo}$ (eV)	Ag—Si $q\Phi_{Bo}$ (eV)
280	0.78	0.74	0.72
300	0.77 (0.81) [13]	0.74 (0.73) [14]	0.72 (0.72) [15]
320	0.76	0.73	0.71
350	0.75	0.72	0.70

The ideality factor *n* was between 1.01—1.03. However, since no characteristic variation was observed in the nature of the diodes with temperature, $n=0.01$ as a permanent value was accepted throughout the evaluation of the real barrier height.

The values of the barrier height $q\Phi_{Bo}$ are listed in Table I for the diodes at different temperatures.

Barrier height determination from *C*—*V* characteristics

Barrier heights have also been determined by capacitance measurements with applied voltage.

The C^{-2} —*V* plots obtained exhibit excellent linearity. From the intercept V_i on the voltage axis the barrier height $q\Phi_{Bn}$ was found using the relation

$$q\Phi_{Bn} = qV_i + qV_n + kT, \quad (6)$$

where qV_n is the distance between Fermi-level and the conduction band edge in bulk Si:

$$qV_n = E_c - E_F = kT \ln \frac{N_C}{N_D}. \quad (7)$$

This expression was calculated for 280, 300, 320, 350 and 370 K, respectively with $N_D = 7 \cdot 10^{16} \text{ cm}^{-3}$.

Values of qV_n and kT are listed in Table II.

The temperature dependence of the C^{-2} —*V* characteristics for Si—Au diodes is presented in Fig. 7.

The C^{-2} —*V* characteristics of Si—Au, Si—Al and Si—Ag diodes at room temperature are plotted in Fig. 8.

Finally the *C*—*V* relationship of a chemically cleaned (“real barrier”) Ag—Si interface is compared in Fig. 9 to that of an “intimate barrier” Ag—Si diode prepared in ultra high vacuum (UHV) with a clean Si surface.

The barrier height values obtained from *C*—*V* measurements are shown in Table III.

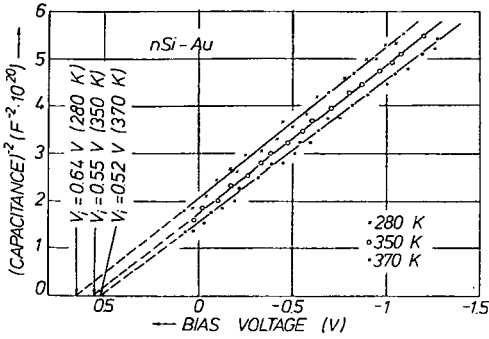


Fig. 7. $C^{-2}-V$ characteristics of nSi(111)—Au contacts at 280, 350 and 370 K

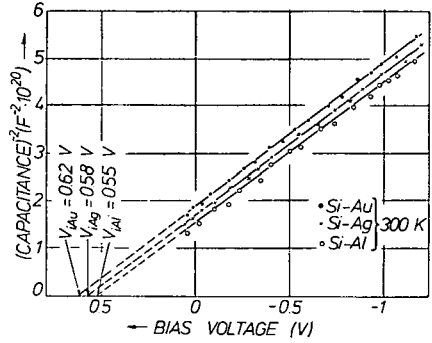


Fig. 8. Comparison of $C^{-2}-V$ characteristics measured on nSi(111)—Au, nSi(111)Ag and nSi(111)—Al contacts at 300 K

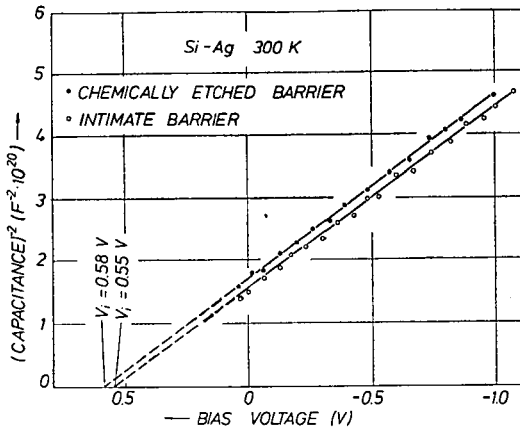


Fig. 9. Comparison of $C^{-2}-V$ characteristics measured on nSi(111) contacts prepared on "chemically cleaned" Si surfaces and on nSi(111)—Ag diodes with "intimate barrier" (prepared by vacuum deposition of Ag on clean Si surface at $5 \cdot 10^{-10}$ mbar)

Table II

Properties of the n type Si samples with $N_D = 7 \cdot 10^{16} \text{ cm}^{-3}$

Temperature (K)	N_b (cm^{-3})	qV_n (eV)	$qV_n + kT$ (eV)
280	$2.52 \cdot 10^{19}$	0.141	0.165
300	$2.80 \cdot 10^{19}$	0.156	0.182
320	$3.08 \cdot 10^{19}$	0.170	0.198
350	$3.53 \cdot 10^{19}$	0.187	0.217
370	$3.84 \cdot 10^{19}$	0.202	0.234

Table III

Barrier heights of n type Si ($N_D = 7 \cdot 10^{18} \text{ cm}^{-3}$) from C-V measurements at various temperatures

Temperature (K)	nSi—Au $q\Phi_{Bn}$ (eV)	nSi—Al $q\Phi_{Bn}$ (eV)	nSi—Ag $q\Phi_{Bn}$ (eV)	
			“REAL BARRIER”	“INTIMATE BARRIER”
280	0.80	—	—	—
300	0.80	0.73	0.76	0.73
320	0.78	—	—	—
350	0.77	0.70	0.72	—
370	0.75	—	—	—

Barrier height determination from photoemission yield measurements

By definition, quantum yield Y is the ratio of the number of photoelectrons and that of the absorbed photons:

$$Y(h\nu) = \frac{I_{ph}(h\nu)/q}{W_a(h\nu)/h\nu}, \tag{8}$$

where I_{ph} is the measured photocurrent, $h\nu$ is the energy of a photon of frequency ν , W_a is the absorbed energy.

Since the absolute values of the yield are not necessary to know, the knowledge of the relative $W_a(h\nu)$ function is sufficient. As a result $Y(h\nu)$ is presented in arbitrary units in Figs. 10—12.

In several papers Y is calculated on the incident radiation power basis only. This gives obviously incorrect results, as reflection, transmission and absorption of light by metallic layers depend on the layer thickness and on the wavelength of light.

This fact was always taken into consideration throughout this work with rigorous calculation of the air-metal-silicon optical layer system. Reflection $R(d, \lambda)$, transmission $T(d, \lambda)$ and absorption $A(d, \lambda)$ were either directly measured or calculated from optical constants found in the literature. In our photoemission experiments monochromatic light was focused onto the metal side of the diodes but checking measurements were also performed with light transmitted

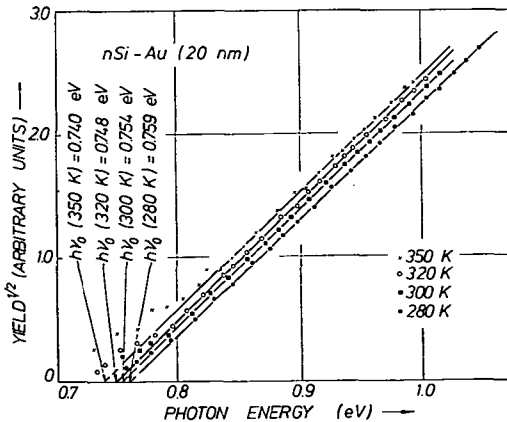


Fig. 10. Photoemission yield-photon energy (“Fowler plots”) on nSi(111)—Au barriers at 280, 300, 320 and 350 K

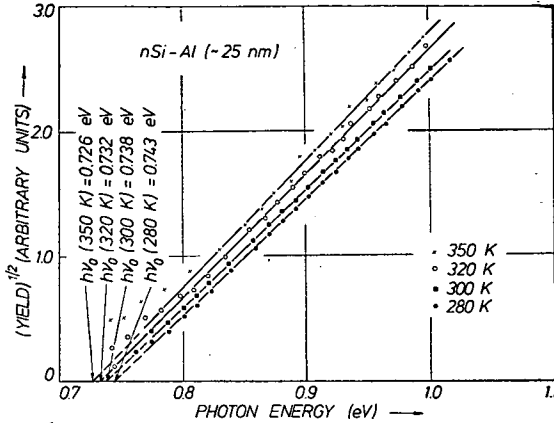


Fig. 11. "Fowler-plots" of nSi(111)—Al diodes at 280, 300, 320 and 350 K

through the silicon towards the metal layer. The fact that no significant deviation was observed for results obtained by the different ways of illumination, verified that the "optical model" used was correct. For metallic layers of thickness $d > 50$ nm, $W_a \approx \{1 - R(d)\} W_i$ is a good approximation for yield calculations, where W_i is the incident energy.

Fig. 10 shows the "Fowler plots" ($Y^{1/2}$ versus $h\nu$) between 280—350 K for nSi—Au diodes at various temperatures.

For nSi—Al and nSi—Ag diodes the Fowler plots are shown in Fig. 11

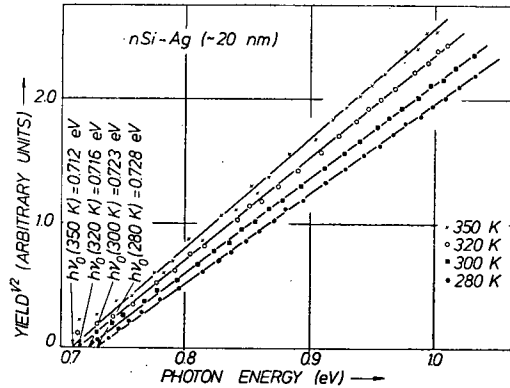


Fig. 12. "Fowler-plots" of nSi(111)—Ag diodes (prepared on "chemically cleaned" nSi) at 280, 300, 320 and 350 K

Table IV

Barrier heights of nSi—Au, nSi—Al and nSi—Ag diodes at various temperatures from photoemission threshold analysis

Temperature (K)	nS—Au $q\Phi_{Bn}$ (eV)	nSi—Al $q\Phi_{Bn}$ (eV)	nSi—Ag $q\Phi_{Bn}$ (eV)
280	0.76	0.74	0.73
300	0.75	0.74	0.72
320	0.75	0.73	0.72
350	0.74	0.73	0.71

and Fig. 12, respectively, at 280, 300, 320, and 350 K temperatures measured by a.c. technique with light chopped at 239 Hz. Table IV shows the barrier height data obtained from photoemission threshold analysis for $n\text{Si}-\text{Au}$, $n\text{Si}-\text{Al}$, and $n\text{Si}-\text{Ag}$ diodes at various temperatures.

*Calculation of the attenuation length of hot electrons
in metallic layers from thickness dependence of the photoemission yield*

The range (or attenuation length) $L(h\nu)$ of hot electrons is defined as follows: When monochromatic light of energy $h\nu$ is incident upon the surface of the metallic layer of thickness d , it can be found both experimentally and theoretically that the number of electrons escaping over the metal-semiconductor barrier at the opposite side of the layer is proportional to $\exp\left\{-\frac{d}{L(h\nu)}\right\}$. $L(h\nu)$ can be determined from the thickness dependence of the external photoemission yield. When $d > 30$ nm, the penetration depth of light is relatively small comparing to thickness, and $L(h\nu)$ can be determined by comparing photoemission yields obtained for thicknesses d_1 and d_2 respectively:

$$L(h\nu) = \frac{d_2 - d_1}{\ln \frac{Y(h\nu, d_1)}{Y(h\nu, d_2)}} \quad (9)$$

if $d_2 > d_1$. $Y(h\nu, d_i)$ is the ratio of the number of emitted electrons and absorbed photons of energy $h\nu$ by the layer of thickness d_i .

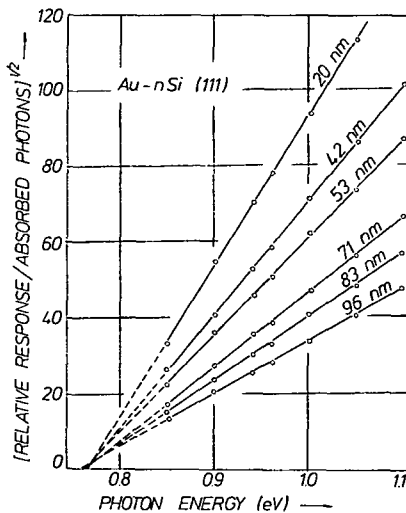


Fig. 13. The dependence of photoresponse on photon energy for 6 different thicknesses (20 nm, 42 nm, 53 nm, 71 nm, 86 nm, 96 nm) of Au deposited on "chemically cleaned" nSi(111) surfaces

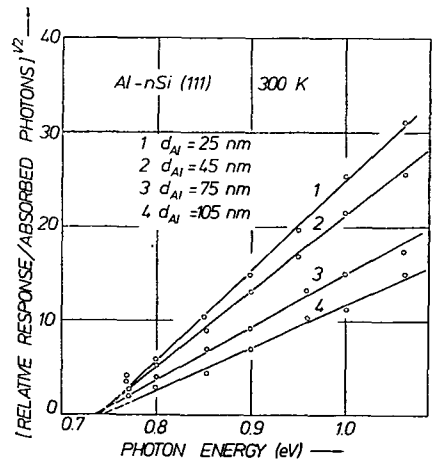


Fig. 14. The dependence of photoresponses on photon energy for 4 different thicknesses (25 nm, 45 nm, 75 nm, 105 nm) of Al deposited on "chemically cleaned" nSi(111) surfaces

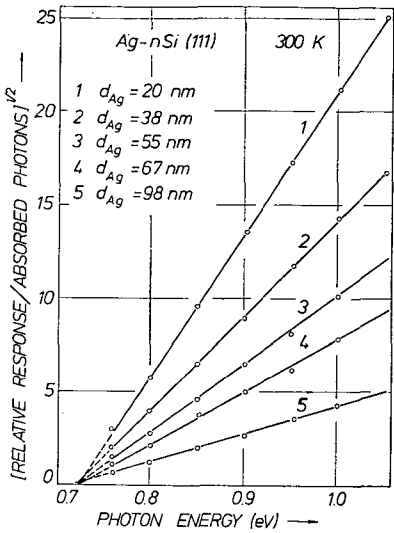


Fig. 15. The dependence of photoresponse on photon energy for 5 different thicknesses (20 nm, 38 nm, 55 nm, 67 nm, 98 nm) of Ag deposited on "chemically cleaned" nSi(111) surfaces

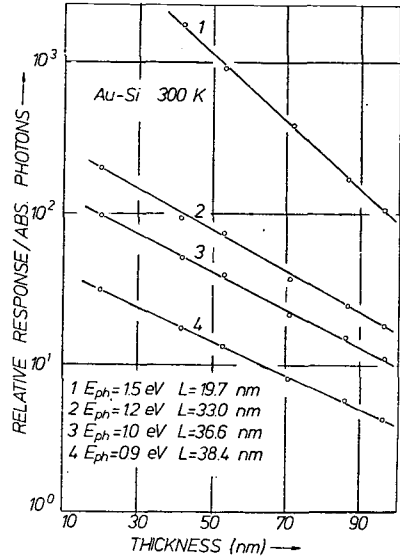


Fig. 16. The photoresponse as a function of the Au film-thicknesses measured at 0.9 eV, 1.0 eV, 1.2 eV and 1.5 eV photon energies for Au-nSi (111) Schottky diodes prepared on "chemically cleaned" Si surfaces.

Fig. 13 shows the photoemission yield of nSi—Au diodes with various layer thickness (20, 42, 53, 71, 86 and 96 nm) measured at room temperature.

The photoemission yield for nSi—Al diodes is presented in Fig. 14 for various layer thicknesses (25, 45, 75 and 105 nm) at 300 K.

Fig. 15 shows the photoemission yield for nSi—Ag diodes with various layer thicknesses (20, 38, 55, 67, and 98 nm) at 300 K.

The graphical determination of $L(h\nu)$ is shown in Fig. 16 at 300 K, for the results plotted in Fig. 14. The same procedure was used to determine graphically the attenuation length $L(h\nu)$ for nSi—Al diodes and nSi—Ag diodes at 300 K.

Table V

Attenuation length $L(h\nu)$ in metallic layers from photoemission measurements for nSi—Au, nSi—Al and nSi—Ag diodes at various temperatures

Temperature (K)	Range of hot electrons $L(h\nu)$ [nm]							
	Au		Al			Ag		
	0.9 eV	1.0 eV	0.8 eV	0.9 eV	1.0 eV	0.8 eV	0.9 eV	1.0 eV
280	39.0	37.2	56.6	51.9	50.2	26.4	25.1	24.5
300	38.4	36.6	55.8	51.0	49.4	25.8	24.7	24.1
320	37.9	36.1	55.0	50.2	48.6	25.0	24.3	23.8
350	37.0	35.3	53.7	49.5	47.6	24.7	23.7	23.3

Thickness dependence of the photoemission yield was also measured at 280, 320 and 350 K for $n\text{Si—Au}$, $n\text{Si—Ag}$ and $n\text{Si—Al}$ diodes. Results of these measurements and attenuation lengths $L(h\nu)$ for $n\text{Si—Au}$, $n\text{Si—Ag}$, and $n\text{Si—Al}$ diodes are assembled in Table V giving the temperature dependence of $L(h\nu)$ for Au, Ag and Al layers.

4. Discussion

Photoemission threshold measurements have been accepted as the most reliable and direct method of determining Schottky-barrier heights. By the use of lock-in detection method, leakage effects caused by tunneling and thermal excitation can be eliminated [9, 11]. A rigorous calculation of the power absorbed by the thin films proved to also be necessary.

Using photoemission, the knowledge of the diode area is not necessary in opposition to the current-voltage ($I-V$) method. The discrepancy obtained between the results of the photoemission and $I-V$ methods can be due to the presence of tunneling current for higher temperature and that of generation — recombination currents for lower temperature [7] and the choice of the effective Richardson — constant A^{**} . However, no significant discrepancy was observed in the experiments which can be explained by the fact that for the relatively high temperature range (280—350 K) thermoemission proves to be the determinant component of the observed current.

Precision of capacitance-voltage ($C-V$) measurements can be considered quite good for “intimate barriers” prepared in UHV and by sophisticated cleaning technique [10] but seemed to be inferior in precision comparing to the photoemission and even to the $I-V$ method in our experiments when diodes were prepared with chemically cleaned Si-surfaces and an intermediate very thin dielectric layer was always present between the metal layer and the semiconductor.

Comparing the barrier height values collected in Tables I, II, and IV, it can be observed that the barrier heights determined by $I-V$ and $C-V$ methods are 0.02 and 0.04 eV respectively larger than those obtained by the photoemission method. However, the results concerning the temperature dependence of barrier height were consistent; $I-V$, $C-V$ and photoemission experiments show the same tendency, i.e. decreasing barrier height values with increasing temperature. The slope $\frac{q\Phi_{Bo}}{\Delta T} = -4 \cdot 10^{-4} \text{ eV/K}$ is in good agreement with the similar slopes of $-3 \cdot 2 \cdot 10^{-4} \text{ eV/K}$ and $-3 \cdot 4 \cdot 10^{-4} \text{ eV/K}$ obtained by photoemission measurements and reported in [9] and [11], respectively.

The values obtained for attenuation length $L(h\nu)$ of hot electrons for Au are in good agreement with those published in [4, 5] but are smaller than those given in [3].

This discrepancy is obviously due to the fact that in [3] the optical absorption, transmission and reflection values were obtained for Au layers deposited on glass substrates: however in the present work and in [4, 5, 8] Au layers were prepared on Si.

The experimentally determined attenuation length L can be expressed by

$$\frac{1}{L} \approx \frac{1}{l_{ee}} + \frac{1}{l_{eph}} \quad (10)$$

if Si is moderately doped, where l_{ee} is the mean free path of electron-electron scattering and l_{eph} is the mean free path of electron-lattice (electron-phonon) interaction.

l_{ee} is independent of temperature but l_{eph} shows strong temperature dependence, and it is proportional to $\frac{1}{T}$ above ~ 20 K. In the temperature range of 280—350 K an empirical relation of $T^{0.23}L(T) = \text{const}$ seems to be correct for Au layers.

* * *

Acknowledgement

The authors wish to acknowledge the assistance of Mr. I. BARSONY.

List of symbols

A :	absorption coefficient
A^{**} :	Richardson constant (amp cm ⁻² K ⁻²)
C :	differential capacitance (F)
d :	layer thickness (cm)
E_c :	energy level of conduction band (eV)
E_F :	Fermi level (eV)
$h\nu$:	photon energy (eV)
I :	current density (amp cm ⁻²)
I_{ph} :	photoelectric current (amp)
I_s :	saturation current (amp)
k :	Boltzmann's constant (joule/K)
L :	attenuation length (range/cm)
N_A :	acceptor concentration (cm ⁻³)
N_D :	donor concentration (cm ⁻³)
q :	charge of electron (coul)
qV_n :	distance between Fermi-level and conduction band (eV)
$q\Phi_{Bo}$:	zero field asymptotic barrier height (eV)
$q\Phi_{Bn}$:	Schottky barrier height on n-type semiconductor (eV)
R :	reflection coefficient
T :	absolute temperature (K)
T :	transmission coefficient
V :	bias voltage (V)
W_a :	absorbed energy (eV)
W_i :	incident energy (eV)
Y :	photoelectric response (yield)
$\Delta\phi$:	Schottky barrier lowering (V)

References

- [1] Mead, C. A.: Solid-State Electron, **9**, 1023 (1966).
- [2] Crowell, C. R., W. G. Spitzer, L. E. Howarth, L. E. Labate: Phys. Rev. **127**, 2006 (1962).
- [3] Sze, S. M., J. L. Moll, T. Sugano: Solid-State Electron. **7**, 509 (1964).
- [4] Joshea, R. W., R. C. Lucas: Phys. Rev. **138**, 1182 (1965).
- [5] Sensik, M., J. M. Seiler: C. R. Acad. Sc. Paris **267**, 1439 (1968).
- [6] Yu, A. Y.: Solid-State Electron. **13**, 97 (1970).
- [7] Thanailakis, A.: J. Phys. C.: Solid State **8**, 655 (1975).

- [8] Seiler, J. M., M. Sensik: C. R. Acad. Sc. Paris 273, 123 (1971).
- [9] Anderson, C. L., C. R. Crowell, T. N. Kao: Solid-State Electron. 18, 705 (1975).
- [10] van Otterloo, J. P., L. J. Gerritsen: J. Appl. Phys. 49, 723 (1978).
- [11] Rideout, V. L.: Thin Solid Films 48, 261 (1978).
- [12] Stuart, K., F. Wooten, W. E. Spicer: Phys. Rev. 135, A 495 (1964).
- [13] Turner, T., E. H. Rhoderick: Solid-State Electron. 11, 291 (1968).
- [14] Strutt, A. K.: Appl. Phys. Lett. 21, 405 (1972).

ИЗМЕРЕНИЕ ВЫСОТЫ БАРЬЕРА И ЗАТУХАЮЩЕГО ПУТИ ГОРЯЧЕГО ЭЛЕКТРОНА НА ДИОДАХ Au—Si, Ag—Si И Al—Si В ТЕМПЕРАТУРНОМ ИНТЕРВАЛЕ 280—350 К

Б. Пелле, Й. Киспетер, Я. Пейснер

Изготавливались Шоттки барьерные диоды с испарением Au—, Ag— и Al-ых слоев на химически очищенном Si типа (*n*) с проводимостью 0,1 ом.см при давлении $5 \cdot 10^{-8}$ мбар. Высота барьера диодов определялась стандартным методом I—V, C—V и методом измерения фотоэмиссионного порога в температурном интервале 280—350 К.

Разными методами измерения определялась одинаковая тенденция. Высота барьера с повышением температуры несколько уменьшается ($-4 \cdot 10^{-4}$ эВ/К). Особое внимание уделили определению точного значения фотоэмиссионной эффективности. Фотоэмиссионные измерения являлись наилучшим методом определения высоты барьера, однако, между результатами полученными фотоэмиссионным методами I—V, C—V нет значительных расхождений. Затухающий путь горячих электронов *L* в серебряном и алюминиевом материалах определялся из результатов измерений фотоэмиссионной эффективности при разных толщинах металлических слоев в температурном интервале 280—350 К. При использовании золотых слоев в температурном интервале 280—350 К установили следующую функциональную зависимость: $T^{0,23} \cdot L(T) = \text{const}$.